J Solution Chem
https://doi.org/10.1007/s10953-018-0729-9

The Study of Solute–Solvent Interactions in 1-Butyl-3-Methylimidazolium Hexafluorophosphate + 2-Pyrrolidone from Volumetric, Acoustic, Optical and Spectral Properties

V. Srinivasa Rao[1,5] · M. Srinivasa Reddy[2] · K. Thomas S. S. Raju[3] · B. L. Rani[4] · B. Hari Babu[5]

Received: 31 March 2017 / Accepted: 16 October 2017

Abstract The density (ρ), speed of sound (u) and refractive index (n_D) of [Bmim][PF_6], 2-pyrrolidone and their binary mixtures were measured over the whole composition range as a function of temperature between (303.15 and 323.15) K at atmospheric pressure. Experimental values were used to calculate the excess molar volumes $\left(V_m^E\right)$, excess partial molar volumes $\left(\overline{V}_m^E\right)$, partial molar volumes at infinite dilution $\left(\overline{V}_m^{E,\infty}\right)$, excess values of isentropic compressibility $\left(\kappa_S^E\right)$, free length $\left(L_f^E\right)$ and speeds of sound $\left(u^E\right)$ for the binary mixtures. The calculated properties are discussed in terms of molecular interactions between the components of the mixtures. The results reveal that interactions between unlike molecules take place, particularly through intermolecular hydrogen bond formation between the C_2–H of [Bmim][PF_6] and the carbonyl group of pyrrolidin-2-one. An excellent correlation between thermodynamic and IR spectroscopic measurements was observed. The observations were further supported by the Prigogine–Flory–Patterson (PFP) theory of excess molar volume.

Keywords [Bmim][PF_6] · 2-Pyrrolidone · Density · Speed of sound · Refractive index · Excess thermodynamic parameters

Electronic supplementary material The online version of this article (https://doi.org/10.1007/s10953-018-0729-9) contains supplementary material, which is available to authorized users.

✉ B. Hari Babu
dr.b.haribabu@gmail.com

[1] Department of Chemistry, SRR & CVR Govt. Degree College, Vijayawada 520008, AP, India

[2] Department of Chemistry, TRR Govt. Degree College, Kandukur 523105, AP, India

[3] Department of Chemistry, Andhra Loyola College, Vijayawada 520008, AP, India

[4] Department of Chemistry, Chalapathi Institute of Engineering and Technology, Guntur 522034, AP, India

[5] Department of Chemistry, Acharya Nagarjuna University, Nagarjunanagar 522510, AP, India

Published online: 16 March 2018

1 Introduction

In recent times, ionic liquids (ILs) have attracted considerable attention because of their distinctive properties such as thermal stability, non-volatility and reusability [1, 2]. ILs can be selected with different anions and cations, so that one can form an ionic liquid with the desired properties. Moreover, ILs had been known for a long time, but their extensive use as solvents in chemical processes for synthesis and catalysis has recently became significant. Two main disadvantages of ILs are that they are very expensive when compared to molecular organic solvents and more viscous than conventional organic solvents, which may hamper their applications. Mixtures of ILs and molecular organic solvents have been gaining the interest of researchers because the resultant liquid mixtures possess advantages over both IL and molecular organic solvents. The properties of these mixtures depend on the mixing ratio. Mixing of the ILs with molecular solvents is one of the steps to minimize the usage of expensive ILs and to save time for preparing new ILs with desired properties [3]. Fortunately, their mixtures with molecular solvents show reduced viscosity without affecting their advantages as green solvents. In particular, the addition of polar co-solvents can strongly influence the physical and chemical properties of ILs such as viscosity, reactivity and electrical conductivity as well as solubility and solvation properties [4]. Hence, IL + molecular solvent mixtures have received growing attention in the past few years. The potential of these new substances can be exploited by studying their properties like volumetric, acoustic and refractive index, etc., because this data is important for industrial applications.

The choice of the ionic liquid, 1-butyl-3-methylimidazolium hexafluoro phosphate ([Bmim][PF_6]), was on the basis of its ability as a green plasticizer for poly(L-lactide) [5], in sequential application in Tussah silk dyeing [6], in RP HPLC [7], in organic synthesis [8], in separation technology [9] and also used in enzymatic catalysis [10]. On the other hand, 2-pyrrolidone (PY) was chosen because of its wide use in applied chemistry, industry and participation in biological processes [11, 12]. A variety of drugs are 2-pyrrolidone derivatives including Cotinine, Doxapram, Piracetam, Povidone, and Ethosuximide. It is also used in inkjet cartridges. Sustainable production of 2-pyrrolidone, used as a building block for active pharmaceutical ingredients, a solvent found in water-based ink and used as a solvent for membrane filters, polymer precursor, etc., is important. The study of the molecular interactions in the binary mixtures of two industrially important solvents, 1-butyl-3-methylimidazolium hexafluoro phosphate and 2-pyrrolidinone can be useful in many industrial applications like organic synthesis, separation technology, etc.

Systematic investigations of the physicochemical properties of [Bmim][PF_6] with molecular organic solvents like *N*,*N*-dimethylformamide [13], methyl methacrylate [14], butanol, acetone [15], THF, DMSO, methanol, acetonitrile [16], ethanol, benzene [17] and 2-propoxyethanol [18] have been reported. However, a literature review indicates that a systematic study of the volumetric, acoustic, optical and spectroscopic properties of binary mixtures of [Bmim][PF_6] with 2-pyrrolidone has not been previously reported. In the present work, we investigate the molecular interactions of [Bmim][PF_6] with 2-pyrrolidone and their affect on the volumetric, acoustic, optical, spectroscopic properties and their derived parameters of [Bmim][PF_6] + 2-pyrrolidone binary mixtures.

On the basis of our initial experiments, [Bmim][PF_6] was found to be totally miscible with PY in all proportions. Hence, in the present study, we measured the densities, speeds of sound and refractive indices of the binary mixtures of [Bmim][PF_6] with PY in the temperature range between 303.15 and 323.15 K over the entire composition range at

atmospheric pressure. Based on the measured values, we calculated the excess/deviation properties needed for their potential application in industrial processes. Here we report excess properties such as molar volumes $\left(V_m^{\mathrm{E}}\right)$, isentropic compressibilities $\left(\kappa_S^{\mathrm{E}}\right)$, free length $\left(L_{\mathrm{f}}^{\mathrm{E}}\right)$, and speeds of sound $\left(u^{\mathrm{E}}\right)$ along with $\left(\frac{\partial V_m^{\mathrm{E}}}{\partial T}\right)_p$ and $\left(\frac{\partial H_m^{\mathrm{E}}}{\partial p}\right)_T$. Also, the deviations of refractive index on the volume fraction basis $(\Delta_\phi n_{\mathrm{D}})$ are reported for the binary mixtures and fitted with the Redlich–Kister polynomial equation. Finally, an attempt has been made to understand the interaction behavior between the two liquids in the mixtures using IR spectroscopy. In addition, analysis of $V_{\mathrm{m}}^{\mathrm{E}}$ data of the present mixtures was done through the Prigogine–Flory–Patterson (PFP) theory.

2 Experimental Section

2.1 Materials

The ionic liquid, [Bmim][PF_6] (CAS174501-64-5), with mass fraction purity 0.99 was used in this work. It was purchased from Iolitec GmBH (Germany), while PY (CAS616-45-5) with mass fraction purity 0.995 was supplied by Sigma–Aldrich. The chemicals used in the present investigation were purified by methods described in the literature [19, 20]. The water content in the IL and PY was determined using a Karl Fisher titrator (Metrohm, 890 Titrando). Before taking any measurement, all samples were dried for at least 72 h under a vacuum (0.1 Pa) and moderate temperature (beginning at room temperature and increasing it gradually over a 6 h period up to 333 K). The water content of all the samples was further checked and found to be less than 150 ppm, a value much lower than the original pre-evacuation analysis, which typically showed values in the range of less than 210 ppm. [Bmim][PF_6] was thus used without further purification, while PY was further purified by distillation. A list of chemicals with details of their provenance, CAS number, and mass fraction purity are given in Table S1 of the supplementary information. The purities were verified by comparing the measured density, speed of sound and refractive index of the pure liquids with the literature values at atmospheric pressure and the results are given in Table 1.

2.2 Apparatus and Procedure

2.2.1 Sample Preparation

lL samples were freshly prepared in amber colored glass vials with screw caps having PFE septa, and were secured sealed with parafilm to prevent absorption of moisture from the atmosphere, and were then stirred for more than 30 min to ensure total dissolution of the mixtures. Samples were taken from the vials with a syringe through the PFE septum. Samples were prepared by weighing with a precision of $\pm$ 0.01 mg, using a Sartorius electronic balance (CPA225D). The uncertainty of the resulting mole fractions of the mixtures was estimated as being $\pm\ 2 \times 10^{-4}$.

Table 1 Comparison of experimental values of density, ρ, speed of sound, u, refractive index, n_D, and specific heat, C_p, of pure liquids with the corresponding literature values at different temperatures and at atmospheric pressure p = 101.3 kPa

Liquid	T (K)	ρ (kg·m^{-3})		u (m·s^{-1})		n_D		C_p (J·K^{-1}·mol^{-1})
		Expt.	Lit.	Expt.	Lit.	Expt.	Lit.	Lit.
[Bmim][PF_6]	303.15	1364.588	1363.277 [14]	1431.66	1430.6 [22]	1.40779	1.40746 [18]	410.33 [23]
	308.15	1360.409	1359.191 [14]	1419.82	1419.00 [22]	1.406474	1.40585 [18]	413.14 [23]
	313.15	1356.239	1355.087 [14]	1408.22	1406.4 [22]	1.405118	1.40468 [18]	415.98 [23]
	318.15	1352.085	1350.980 [14]	1396.84	1395.50 [21]	1.403706	1.40352 [18]	418.91 [23]
	323.15	1347.953	1346.874 [14]	1385.63	1385.155 [21]	1.402342	1.40243 [18]	421.88 [23]
2-Pyrrolidinone	303.15	1103.073	1103.07 [25] 1103.17 [26]	1617.97	1617.71 [25]	1.484032	1.48403 [25]	171.33 [24]
	308.15	1098.989	1098.99 [25] 1099.13 [26]	1601.62	1601.32 [25]	1.482177	1.48218 [25]	172.57 [24]
	313.15	1094.903	1094.90 [25] 1095.18 [26]	1585.44	1585.44 [25]	1.48033	1.48033 [25]	173.91 [24]
	318.15	1090.823	1090.82 [25] 1091.01 [26]	1569.39	1570.39 [25]	1.47412	1.47841 [25]	175.10 [24]
	323.15	1086.745	1086.75 [25]	1553.48	1553.48 [25]	1.476486	1.47649 [25]	176.31 [24]

Standard uncertainties u are: $u(\rho)$ = 1.0 kg·m^{-3}, $u(u)$ = 0.5 m·s^{-1}, $u(n_D)$ = 0.00005, $u(T)$ = 0.01 K and $u(p)$ = 0.5 kPa

2.2.2 Measurement of Density and Speed of Sound

Densities and speed of sound were measured with an Anton Paar DSA-5000 M vibrating-tube density and sound velocity meter. The density meter was calibrated with doubly distilled degassed water, and with dry air at atmospheric pressure. The temperature of the apparatus was controlled to within ± 0.01 K by a built-in Peltier device. Measured density and speed of sound values (at a frequency of approximately 3 MHz) are precise to 5×10^{-3} kg·m^{-3} and 5×10^{-1} m·s^{-1}, respectively. The standard uncertainties associated with the measurements of temperature, density and speed of sound are estimated to be ± 0.01 K, 5×10^{-2} kg·m^{-3} and ± 0.5 m·s$^{-1,}$ respectively.

2.2.3 Measurement of Refractive Index

The refractive indices were determined using an automatic refractometer (Anton Paar Dr Krenchen Abbemat (WR-HT)) which also has a temperature controller that keeps the samples at working temperature. The uncertainties in the temperature and refractive index values are ± 0.01 K and ± 5×10^{-5}, respectively. The apparatus was calibrated by measuring the refractive index of Millipore quality water and tetrachloroethylene (supplied by the company) before each series of measurements according to the manual instructions. The calibration was checked with pure liquids having known refractive indices.

2.2.4 Measurement of Infrared Spectra

Infrared transmittance was measured using a Shimadzu Fourier transform infrared (FT-IR) spectrometer (IRAffinity-1S) equipped with attenuated total reflectance (ATR) accessories. The spectral region was 650–4000 cm^{-1} with resolution of 2 cm^{-1} and 100 scans were taken. At least five repeated measurements were performed for each sample.

3 Results and Discussion

The experimentally measured density (ρ), speed of sound (u) and refractive index (n_D) results for the binary mixtures of [Bmim][PF_6] with PY at different temperatures are given in Table 2. The IR spectral data was recorded at room temperature. The changes in values of ρ, u and n_D with respect to mole fraction are non-linear at all studied temperatures, whereas the changes in their values with respect to temperature are linear. This trend indicates the existence of molecular interactions between the liquids under study at all studied temperatures. The excess and deviation parameters were calculated from the experimental data using well-known thermodynamic expressions given elsewhere [27]. The Redlich–Kister polynomial coefficients of the computed excess properties and corresponding standard deviations are presented in Table S2 of the supporting information.

The variations observed in these excess/deviation parameters are due to the resultant contribution of several opposing effects, namely chemical, structural, and physical [28]. The chemical or specific interactions include hydrogen bonding between component molecules and charge-transfer complexes. The structural contributions are such as interstitial accommodation and geometrical fitting of one component into another. Excess molar volumes for the binary mixtures of [Bmim][PF_6] with PY as a function of composition from T = 303.15–323.15 K are shown in Fig. 1. The curves in the figure have a sigmoid

Table 2 Experimental density (ρ), speed of sound (u), refractive index (n_D), molar volume (V_m), isentropic compressibility (κ_s), free length (L_f) and isobaric thermal expansion coefficient (α_p) with mole fraction (x_1) of [Bmim][PF_6] in the binary liquid mixture of {[Bmim][PF_6] + 2-pyrrolidinone} from T/K = 303.15–323.15 at pressure p = 101.3 kPa

x_1	ρ (kg·m^{-3})	u (m·s^{-1})	n_D	V_m (10^{-6} m^3·mol^{-1})	κ_s (10^{-10} Pa^{-1})	L_f (10^{-11} m)	α_p (10^{-4} K^{-1})
303.15 K							
0.0000	1103.07	1617.97	1.48403	77.16	3.463	3.862	7.41
0.0494	1134.15	1584.68	1.47539	83.72	3.511	3.889	6.54
0.1025	1161.46	1575.15	1.46743	90.84	3.470	3.866	6.17
0.1503	1182.17	1566.55	1.46088	97.31	3.447	3.853	6.06
0.2215	1209.05	1553.76	1.45232	106.86	3.426	3.842	6.03
0.3376	1249.12	1532.89	1.44097	121.95	3.407	3.831	6.00
0.4502	1281.92	1512.66	1.43229	136.30	3.409	3.832	5.91
0.5654	1309.38	1491.96	1.42521	150.96	3.431	3.845	5.82
0.6527	1326.07	1476.26	1.42077	162.17	3.460	3.861	5.76
0.7421	1339.46	1460.19	1.41683	173.84	3.501	3.884	5.68
0.8295	1348.94	1446.49	1.41345	185.51	3.543	3.907	5.63
0.8622	1351.84	1442.61	1.41227	189.93	3.554	3.913	5.63
0.9019	1355.19	1438.47	1.41089	195.30	3.566	3.920	5.67
0.9495	1359.38	1434.92	1.40932	201.66	3.573	3.923	5.81
1.0000	1364.59	1431.66	1.40779	208.26	3.575	3.925	6.14
308.15 K							
0.0000	1098.99	1601.62	1.48218	77.44	3.547	3.944	7.43
0.0494	1130.43	1569.09	1.47367	83.99	3.593	3.970	6.64
0.1025	1157.89	1560.04	1.46577	91.12	3.549	3.945	6.30
0.1503	1178.59	1551.84	1.45925	97.60	3.523	3.931	6.20
0.2215	1205.38	1539.60	1.45075	107.19	3.500	3.918	6.16
0.3376	1245.37	1519.50	1.43947	122.31	3.478	3.906	6.10
0.4502	1278.13	1499.87	1.43084	136.70	3.478	3.906	6.00
0.5654	1305.56	1479.62	1.42380	151.40	3.499	3.917	5.91
0.6527	1322.25	1464.16	1.41939	162.64	3.528	3.934	5.85
0.7421	1335.64	1448.25	1.41547	174.34	3.570	3.957	5.77
0.8295	1345.14	1434.60	1.41211	186.04	3.612	3.980	5.70
0.8622	1348.02	1430.72	1.41094	190.47	3.624	3.987	5.69
0.9019	1351.33	1426.56	1.40956	195.86	3.636	3.994	5.71
0.9495	1355.39	1422.97	1.40800	202.26	3.644	3.998	5.83
1.0000	1360.41	1419.82	1.40647	208.90	3.646	3.999	6.14
313.15 K							
0.0000	1094.90	1585.44	1.48033	77.73	3.633	4.028	7.46
0.0494	1126.64	1553.66	1.47197	84.27	3.677	4.052	6.74
0.1025	1154.21	1545.09	1.46409	91.41	3.629	4.025	6.43
0.1503	1174.91	1537.31	1.45761	97.91	3.601	4.010	6.34
0.2215	1201.61	1525.63	1.44916	107.52	3.576	3.996	6.29
0.3376	1241.54	1506.30	1.43795	122.69	3.550	3.981	6.20
0.4502	1274.25	1487.28	1.42937	137.12	3.548	3.980	6.09

Table 2 continued

x_1	ρ (kg·m^{-3})	u (m·s^{-1})	n_D	V_m (10^{-6} m^3·mol^{-1})	κ_s (10^{-10} Pa^{-1})	L_f (10^{-11} m)	α_p (10^{-4} K^{-1})
0.5654	1301.66	1467.48	1.42237	151.86	3.567	3.991	6.00
0.6527	1318.34	1452.26	1.41798	163.12	3.597	4.007	5.94
0.7421	1331.75	1436.50	1.41408	174.85	3.639	4.031	5.86
0.8295	1341.27	1422.91	1.41074	186.58	3.682	4.055	5.77
0.8622	1344.17	1419.03	1.40956	191.02	3.695	4.062	5.75
0.9019	1347.47	1414.85	1.40820	196.42	3.707	4.069	5.76
0.9495	1351.47	1411.21	1.40665	202.84	3.715	4.073	5.86
1.0000	1356.24	1408.22	1.40512	209.54	3.718	4.074	6.13
318.15 K							
0.0000	1090.82	1569.39	1.47841	78.02	3.722	4.113	7.48
0.0494	1122.77	1538.38	1.47018	84.56	3.763	4.136	6.83
0.1025	1150.44	1530.28	1.46234	91.71	3.712	4.107	6.56
0.1503	1171.13	1522.90	1.45591	98.22	3.682	4.090	6.48
0.2215	1197.78	1511.76	1.44752	107.87	3.653	4.075	6.42
0.3376	1237.66	1493.20	1.43638	123.08	3.624	4.058	6.30
0.4502	1270.34	1474.77	1.42786	137.54	3.619	4.056	6.17
0.5654	1297.74	1455.43	1.42089	152.31	3.638	4.066	6.08
0.6527	1314.42	1440.46	1.41651	163.61	3.667	4.082	6.03
0.7421	1327.83	1424.85	1.41263	175.36	3.710	4.106	5.95
0.8295	1337.36	1411.33	1.40930	187.12	3.754	4.130	5.84
0.8622	1340.28	1407.45	1.40814	191.57	3.766	4.137	5.81
0.9019	1343.59	1403.26	1.40678	196.98	3.780	4.145	5.81
0.9495	1347.53	1399.57	1.40523	203.44	3.789	4.149	5.88
1.0000	1352.09	1396.84	1.40371	210.19	3.791	4.150	6.13
323.15 K							
0.0000	1086.75	1553.48	1.47649	78.32	3.813	4.199	7.50
0.0494	1118.92	1523.19	1.46840	84.86	3.852	4.221	6.93
0.1025	1146.67	1515.58	1.46059	92.01	3.797	4.190	6.70
0.1503	1167.36	1508.60	1.45419	98.54	3.764	4.172	6.62
0.2215	1193.93	1498.02	1.44588	108.22	3.732	4.155	6.55
0.3376	1233.75	1480.24	1.43483	123.47	3.699	4.136	6.40
0.4502	1266.40	1462.42	1.42635	137.97	3.692	4.132	6.26
0.5654	1293.77	1443.55	1.41943	152.78	3.709	4.142	6.17
0.6527	1310.45	1428.83	1.41508	164.11	3.738	4.158	6.12
0.7421	1323.87	1413.40	1.41122	175.89	3.781	4.182	6.04
0.8295	1333.43	1399.96	1.40791	187.67	3.826	4.207	5.91
0.8622	1336.36	1396.09	1.40676	192.13	3.839	4.214	5.87
0.9019	1339.68	1391.89	1.40541	197.56	3.853	4.221	5.85
0.9495	1343.57	1388.17	1.40386	204.04	3.862	4.226	5.90

Table 2 continued

x_1	ρ (kg·m^{-3})	u (m·s^{-1})	n_D	V_m (10^{-6} m^3·mol^{-1})	κ_s (10^{-10} Pa^{-1})	L_f (10^{-11} m)	α_p (10^{-4} K^{-1})
1.0000	1347.95	1385.63	1.40234	210.83	3.864	4.227	6.12

Standard uncertainties u are: $u(x_1) = 0.0001$, $u(\rho) = 1$ kg·m^{-3}, $u(u) = 0.5$ m·s^{-1}, $u(n_D) = 0.00005$, $u(T) = 0.01$ K and $u(p) = 0.5$ kPa. Combined uncertainties (confidence level, 95%): U_c (V_m) = $\pm$ 0.01 $\times$ 10^{-6} m^3·mol^{-1}, U_c (κ_s) = $\pm$ 0.01 $\times$ 10^{-10} Pa^{-1}, U_c (L_f) = $\pm$ 0.004 $\times$ 10^{-11} m, U_c (α_p) = $\pm$ 0.02 $\times$ 10^{-4} K^{-1}. All the experiments were carried out at atmospheric pressure

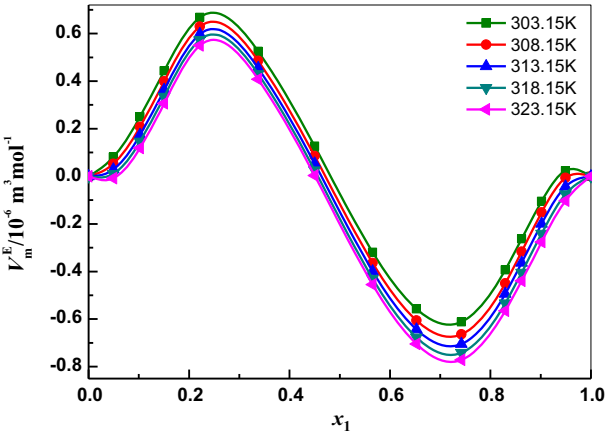

Fig. 1 Plots of excess molar volume $\left(V_m^E\right)$ against mole fraction of [Bmim][PF_6] with PY at different temperatures

shape at all temperatures with positive V_m^E values in the PY rich region and negative V_m^E values in the IL rich region. The present observations of V_m^E can be explained based on microscopic structural changes in the binary system. In the pure state, PY molecules exist as cyclic dimers due to intermolecular hydrogen bonding. This prevents fitting of PY molecules (dimers) into the voids of [Bmim][PF_6], which leads to positive excess molar volumes in the PY rich region. In the IL rich region, the dimeric structure of PY molecules is disturbed in such a way that breakage of intermolecular H bond occurs and consequently more favorable fitting of the smaller PY molecules (monomers) takes place into the voids created by the larger [Bmim][PF_6] molecules, giving rise to negative V_m^E values. In addition to the geometrical fitting, inter molecular hydrogen bond formation between the carbonyl oxygen of PY and C_2-H/$C_{4,5}$-H of $[Bmim]^+$ is also responsible for the strong interactions between solute and solvent in the IL rich region. A similar type of behavior for V_m^E is observed for the rest of studied temperatures. Moreover, the variation of V_m^E for the present system as a function of temperature becomes more negative with rise in temperature in the IL rich region. This is because of the fact that there is more favorable fitting of the smaller PY molecules into the voids created by larger IL molecules, thereby resulting in shrinkage of the volume of the mixture to a larger extent, resulting in more negative V_m^E values with rise in temperature. Therefore, the strength of interaction is enhanced with rise in temperature.

The existing molecular interactions in the current binary system are properly reflected in the properties of partial molar volumes of the constituent molecules. A partial molar volume is the contribution that a component of a mixture makes to the total volume of the solution. Therefore, the partial molar volume is a function of mixture composition. The partial molar volumes $\overline{V}_{m,1}$ of component 1 ([Bmim][PF_6]) and $\overline{V}_{m,2}$ of component 2 (PY) in the mixtures over the whole composition range have been computed using the relationships given elsewhere [29].

The calculated values of $\overline{V}_{m,1}$ and $\overline{V}_{m,2}$ for the studied binary system are presented in Table S3 of the supporting information. From the table, it is evident that the values of $\overline{V}_{m,1}$ ([Bmim][PF_6]) are bigger in the PY rich region than its individual molar volumes in the pure state, which reveals expansion of the volume in the PY rich region and contraction of the volume in the IL rich region when [Bmim][PF_6] is mixed with PY. In the case of $\overline{V}_{m,2}$ (PY), the values are bigger than its individual molar volumes over the entire composition range, which reveals expansion of the volume of PY upon mixing with [Bmim][PF_6]. Figures 2 and 3 illustrate the disparity of excess partial molar volumes of $\overline{V}^{\mathrm{E}}_{m,1}$ ([Bmim][PF_6]) and $\overline{V}^{\mathrm{E}}_{m,2}$ (PY), respectively, in the binary mixtures at T = (303.15, 308.15, 313.15, 318.15 and 323.15) K. These figures not only show the variation of attractive forces between the unlike molecules but also support the inferences drawn from the excess molar volume.

The partial molar volumes $\left(\overline{V}^{\infty}_{m,1},\ \overline{V}^{\infty}_{m,2}\right)$ and excess partial molar volumes at infinite dilution $\left(\overline{V}^{\mathrm{E},\infty}_{m,1},\ \overline{V}^{E,\infty}_{m,2}\right)$ of [Bmim][PF_6] and PY were calculated. The pertinent $\overline{V}^{\infty}_{m,1}$, $\overline{V}^{\infty}_{m,2}$ and $\overline{V}^{\mathrm{E},\infty}_{m,1}$, $\overline{V}^{\mathrm{E},\infty}_{m,2}$ values are presented in Table 3 at T = (303.15, 308.15, 313.15, 318.15 and 323.15) K. Excess partial molar volumes at infinite dilution are of specific interest to understand the solute–solvent interactions, as solute–solute interactions are assumed to have disappeared at infinite dilution. Positive values of $\overline{V}^{\mathrm{E},\infty}_{m,1}$ (at 303.15 K) in the mixtures suggest weaker interactions between ions of [Bmim][PF_6] and PY molecules because of the existence of inter molecular hydrogen bonds in PY. Positive $\overline{V}^{\mathrm{E},\infty}_{m,2}$ values for PY at (303.15, 308.15, 313.15) K are attributed to an ion solvation process and termination of

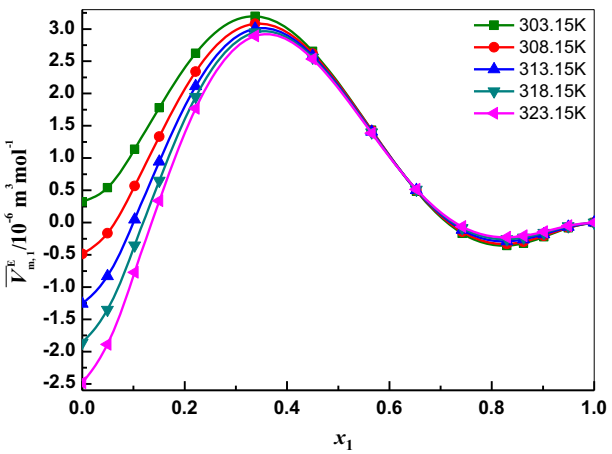

Fig. 2 Plots of excess partial molar volume $\overline{V}^{\mathrm{E}}_{m,1}$ against mole fraction of [Bmim][PF_6] with PY at different temperatures

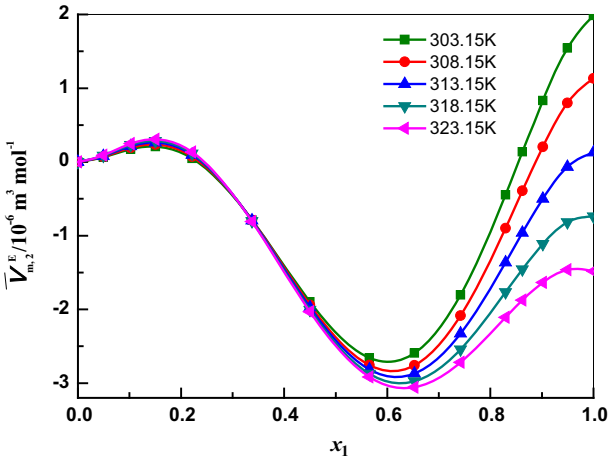

Fig. 3 Plots of excess partial molar volume $\overline{V}^{E}_{m,2}$ against mole fraction of [Bmim][PF_6] with PY at different temperatures

Table 3 Partial molar volumes at infinite dilution ($\overline{V}^{\infty}_{m,1}$, $\overline{V}^{\infty}_{m,2}$) and excess partial molar volumes at infinite dilution ($\overline{V}^{E,\infty}_{m,1}$, $\overline{V}^{E,\infty}_{m,2}$) of [Bmim][$PF_6$] and 2-pyrrolidinone T = (303.15, 308.15, 313.15, 318.15 and 323.15) K

Temp (K)	$\overline{V}^{\infty}_{m,1}$ (10^{-6} m^3·mol^{-1})	$\overline{V}^{E,\infty}_{m,1}$	$\overline{V}^{\infty}_{m,2}$ (10^{-6} m^3·mol^{-1})	$\overline{V}^{E,\infty}_{m,2}$
303.15	208.58	0.32	79.14	1.98
308.15	208.41	− 0.49	78.58	1.13
313.15	208.28	− 1.26	77.86	0.13
318.15	208.32	− 1.86	77.29	− 0.74
323.15	208.35	− 2.49	76.83	− 1.48

Combined uncertainties (confidence level, 95%): $U\left(\overline{V}^{E,\infty}_{m,1}\right) = \pm 0.02 \times 10^{-6}$ m^3·mol^{-1}, $U\left(\overline{V}^{E,\infty}_{m,2}\right) = \pm 0.02 \times 10^{-6}$ m^3·mol^{-1}

ion–ion interactions in [Bmim][PF_6]. As the temperature increases, both $\overline{V}^{E,\infty}_{m,1}$ and $\overline{V}^{E,\infty}_{m,2}$ values decrease and become negative. The decrease in $\overline{V}^{E,\infty}_{m,1}$ and $\overline{V}^{E,\infty}_{m,2}$ values with rise in temperature indicates an increase in the strength of attractions between solute and solvent molecules, which further supports the observed trends in V^{E}_{m} values for the binary system.

In Fig. 4 the κ^{E}_{S} values for [Bmim][PF_6] + PY are seen to be negative except in the PY rich region at all investigated temperatures. The negative κ^{E}_{S} values are attributed to the strong attractive interactions between the molecules of the components [29]. This supports the inference drawn from V^{E}_{m}. The intermolecular free length indicates closer approach of unlike molecules. The trends of the L^{E}_{f} values (Fig. 5) are similar to κ^{E}_{S} at all investigated temperatures. Negative values of L^{E}_{f} are generally explained as being due to the dominance of specific interactions between unlike molecules in the liquid mixture and also due to the structural readjustments in the liquid mixtures towards a less compressible phase of fluid and closer packing of the molecules [29]. Figure 6 shows that the u^{E} values are positive for

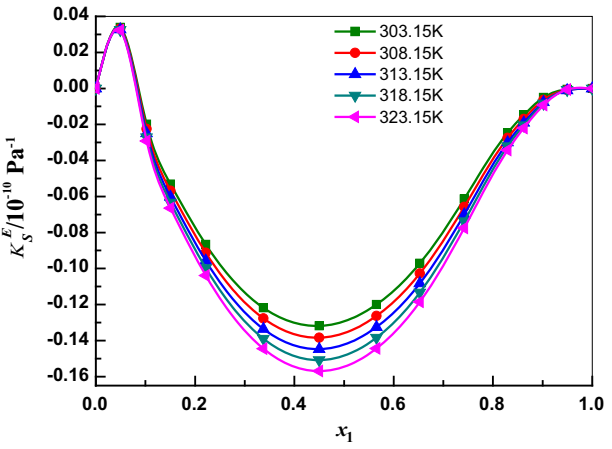

Fig. 4 Plots of excess isentropic compressibility K_S^E against mole fraction of [Bmim][PF_6] with PY at different temperatures

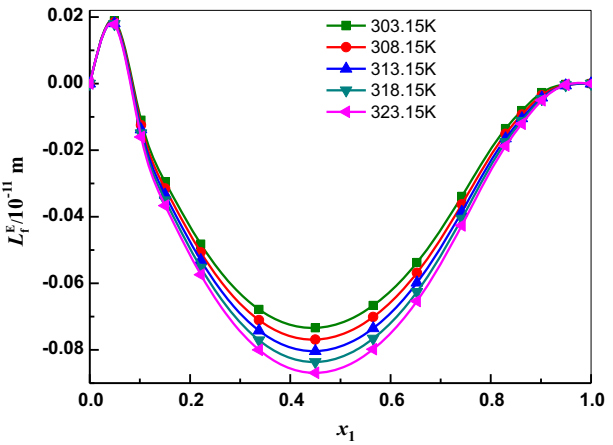

Fig. 5 Plots of excess free length L_f^E against mole fraction of [Bmim][PF_6]with PY at different temperatures

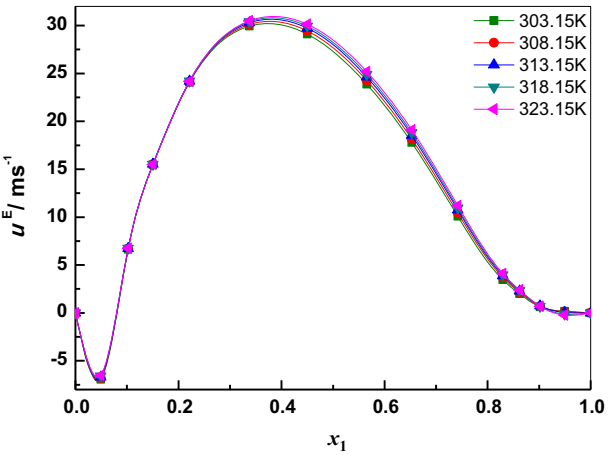

Fig. 6 Plots of excess ultrasonic speed of sounds (u^E) against mole fraction of [Bmim][PF_6] with PY at different temperatures

the system except in the PY rich region at all the studied temperatures. Positive deviations indicate an increasing strength of interaction between the component molecules of the binary liquid mixtures [30]. The refractive indices (n_D) for the binary mixtures at the studied temperatures over the whole composition range are given in Table 2; the values increase with increase in the concentration of the ILs in the mixtures and decrease as the temperature increases for a particular concentration of [Bmim][PF_6]. The values of $\Delta_\phi n_D$ are positive over the range of composition (Fig. 7), which may be attributed to the non-availability of the free volume in the mixture in comparison with the corresponding ideal mixtures [31].

This further supports the existence of strong interactions between the constituent molecules in the binary liquid solutions. The values of the excess functions $\left(\frac{\partial V_m^E}{\partial T}\right)_p$ and $\left(\frac{\partial H_m^E}{\partial p}\right)_T$ are given in Table 4. The variation of $\left(\frac{\partial V_m^E}{\partial T}\right)_p$ and $\left(\frac{\partial H_m^E}{\partial p}\right)_T$ are similar with mole fraction and temperature but with opposite sign. The negative values of $\left(\frac{\partial V_m^E}{\partial T}\right)_p$ for the studied mixtures may be due to the strong interactions existing between the unlike molecules of the mixtures [31]. The isothermal pressure coefficient of excess molar enthalpy $\left(\frac{\partial H_m^E}{\partial p}\right)_T$ has positive values over the whole composition range. This reflects an increase in attraction forces between the two components of these mixtures caused by increasing pressure. Hence, contraction in the volume of the mixture is still possible by increasing the pressure [29, 32].

3.1 Infrared Spectral Studies

The existence of interactions in the system, which were inferred from the above excess/deviation parameters, is well supported by the IR spectral studies. The unique properties of imidazolium cations are found in their electronic structure. The hydrogen in C_2-H is more acidic than for C_4-H and C_5-H due to the electron deficiency in the C=N bond. The resultant acidity of the hydrogen atoms is key to understanding the properties of these ionic

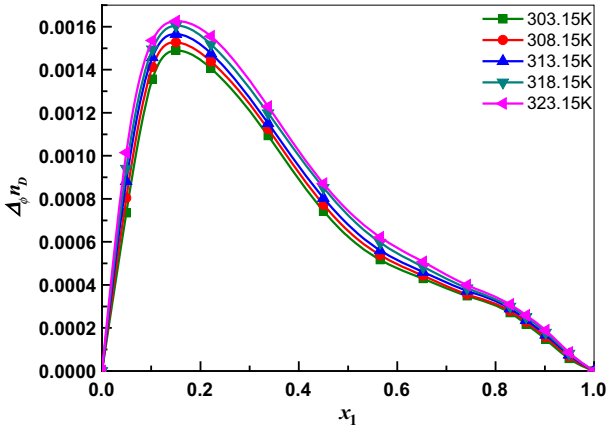

Fig. 7 Plots of deviation in refractive index $\Delta_\phi n_D$ against mole fraction of [Bmim][PF_6] with PY at different temperatures

Table 4 The values of excess functions $\left(\frac{\partial V_m^E}{\partial T}\right)_p$ and $\left(\frac{\partial H_m^E}{\partial p}\right)_T$ at 298.15 K as a function of mole fraction of [Bmim][PF_6]

x_1	$\left(\frac{\partial V_m^E}{\partial T}\right)_p$ (10^{-9} $m^3 \cdot mol^{-1} \cdot K^{-1}$)	$\left(\frac{\partial H_m^E}{\partial p}\right)_T$ (10^{-6} $J \cdot mol^{-1} \cdot Pa^{-1}$)
0.0000	0.00	0.00
0.0494	− 5.92	1.88
0.1025	− 8.42	2.80
0.1503	− 8.89	3.14
0.2215	− 8.46	3.23
0.3376	− 7.94	2.93
0.4502	− 8.47	2.69
0.5654	− 9.32	2.50
0.6527	− 9.99	2.47
0.7421	− 10.86	2.68
0.8295	− 11.47	3.08
0.8622	− 11.27	3.15
0.9019	− 10.27	3.01
0.9495	− 7.16	2.19
1.0000	0.00	0.00

Standard uncertainties u are: $u(x_1) = 0.0002$, $u(T) = 0.01$ K and $u(p) = 0.5$ kPa

Combined uncertainties (confidence level, 95%): $U\left(\left(\frac{\partial V_m^E}{\partial T}\right)_p\right) = \pm\ 0.1 \times 10^{-9}$ $m^3 \cdot mol^{-1} \cdot K^{-1}$, $U\left(\left(\frac{\partial H_m^E}{\partial p}\right)_{T=298.15K}\right) = \pm\ 0.06 \times 10^{-6}$ $J \cdot mol^{-1} \cdot Pa^{-1}$

liquids. The hydrogen on the C_2 carbon (C_2-H) has been shown to bind typically with solute molecules [33, 34].

In order to study the effects of molecular interactions, the infrared absorbance was recorded from 650 to 4000 cm^{-1} (Fig. S1 of the supporting information and Table 5). In the $[Bmim]^+$ cation, the C–H stretching region from 2800 to 3200 cm^{-1} was investigated. The signals in this region can be separated into two parts: signals between 3000 and 3200 cm^{-1} can be attributed to C–H vibrational modes mainly arising from the aromatic imidazolium ring, from the C_2–H and $C_{4,5}$–H stretching frequencies [35]. The signals between 2800 and 3000 cm^{-1} are due to aliphatic C–H groups in the methyl and butyl moieties [36–38]. The C_2–H vibrational frequency (3124.5 cm^{-1}) is shifted to lower frequencies by about 45.4 cm^{-1} when compared to the C_4–H and C_5–H stretches (3169.9 cm^{-1}) because of its stronger acidic character. In the present mixtures, the C_2–H and $C_{4,5}$–H stretching frequencies of the cation are analyzed (Fig. 8). The experimental ATR-IR spectra for PY for the N–H stretching and C=O stretching (Fig. 8) of the amide spectral regions are reported. A wide peak with a maximum at 3228.0 cm^{-1} for the N–H stretching (hydrogen bonded) and a narrower peak at 1688.2 cm^{-1}, corresponding C=O stretching of the amide region of pure PY, are observed. The absence of a peak around 3430.0 cm^{-1} (free N–H) shows that there is no presence of monomeric, nonassociated, PY molecules in its pure state. PY molecules are self-associated through hydrogen bonding and exist as a cyclic dimer (Fig. 9) in its pure state [39].

Table 5 Infrared absorbance wave numbers between 2800 and 3200 cm^{-1} of [Bmim][PF_6] in PY at room temperature and atmospheric pressure p = 101.3 kPa

Mole fraction of [Bmim][PF_6]	Mole fraction of PY	C_2–H stretching	$C_{4,5}$–H stretching	Free N–H stretch	C=O stretch
1.0000	0.0000	3124.5	3169.9	–	–
0.9019	0.0981	3123.5	3169.2	–	1666.1
0.8295	0.1705	3123.2	3168.8	3433.8	1667.8
0.7421	0.2579	3122.8	3168.7	3432.1	1674.8
0.6527	0.3473	3122.3	3168.5	3432.5	1678.8
0.5654	0.4346	3121.2	3168.4	3431.2	1681.1
0.4502	0.5498	3119.8	3167.8	3430.9	1683.7
0.3376	0.6624	3118.2	3167.2	3430.6	1685.3
0.2215	0.7785	3115.1	3167.1	3428.7	1686.5
0.1025	0.8975	–	–	3428.1	1687.1
0.0000	1.0000	–	–	3424.9	1688.2

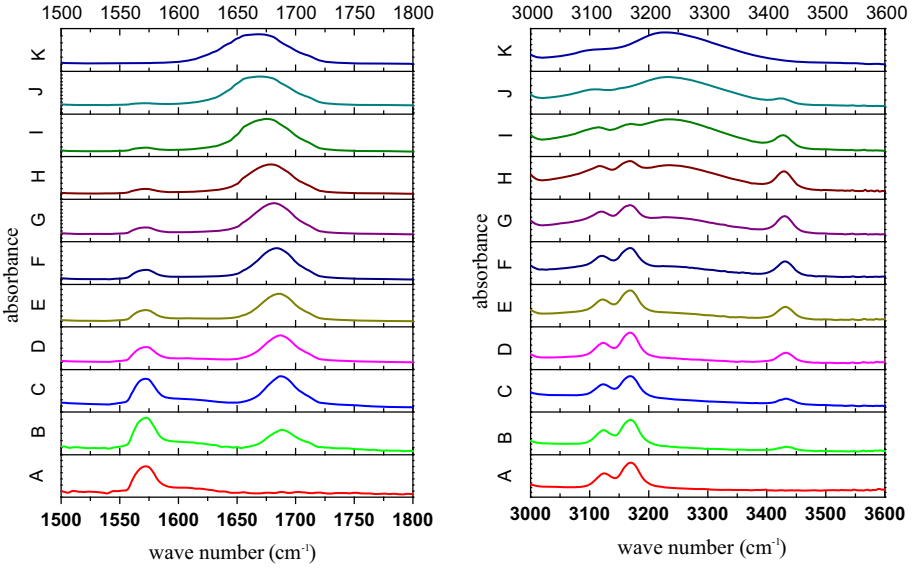

Fig. 8 Infrared spectra between 1500 and 1800 cm^{-1} and between 3000 and 3600 cm^{-1} of: (A) pure IL [Bmim][PF_6]; (B) 0.9019; (C) 0.8295; (D) 0.7421; (E) 0.6527; (F) 0.5654; (G) 0.4502; (H) 0.3376; (I) 0.2215; (J) 0.1025 and (K) pure PY where. (B–J) are the the mole fraction of [Bmim][PF_6] in PY

As the mole fraction of PY increases, an observed red shift in the C_2–H and $C_{4,5}$–H stretching frequencies indicates the formation of a hydrogen bond between $[Bmim]^+$ and PY. The red shift is very predominant in the C_2–H frequencies when compared to the $C_{4,5}$–H stretching frequencies, which indicates that the more acidic C_2–H plays a major role in the formation of a hydrogen bond with the carbonyl oxygen of PY (Fig. 10). Simultaneously, a clear blue shift in C=O Sym Stretch frequencies is observed because of

Fig. 9 Dimeric structure of PY

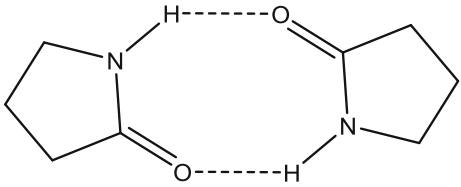

the breakup of strong hydrogen bonds in the cyclic dimeric PY. A wide peak with a maximum at 3228.0 cm^{-1} for the N–H stretching belonging to the cyclic dimer appears in the PY rich region only. As the mole fraction of IL increases it gradually disappears and a sharp peak around 3430.0 cm^{-1} appears that is assigned to free N–H. This also indicates that the N–H proton has no role in the formation of hydrogen bonds in the mixtures.

By examining the ATR-FTIR, it can be concluded that hydrogen bonds exist extensively in such systems which play a key role towards the miscibility and stability of the [Bmim][PF_6] + PY binary system. Hence, it can be assumed that the cyclic dimer in the PY rich region is responsible for the expansion of volume and contraction in the IL rich region because of hydrogen bond formation between the ionic liquid [Bmim][PF_6] and PY.

3.2 Prigogine–Flory–Patterson Statistical Theory for Excess Molar Volume V_m^E

The Prigogine–Flory–Patterson (PFP) theory may be used to analyze and correlate the experimental excess molar volumes of binary mixtures [40, 41]. We have correlated V_m^E of the binary mixtures using PFP theory over the entire range of mole fractions at T = 303.15–323.15 K. The PFP theory considers V_m^E as having three different contributions [42–44]: (i) an interaction contribution V_{int}^E, which is associated with intermolecular specific interactions according to the sign of H_m^E, (ii) a free volume contribution V_{fv}^E, which is associated with the reduced volume-to-reduced temperature ratio with a negative sign, and (iii) an internal pressure contribution,$V_{p^*}^E$, which is associated with breaking of the IL structure upon introduction of molecular organic solvents and changes in the reduced

Fig. 10 Inter molecular hydrogen bonded structure between [Bmim][PF_6] and PY

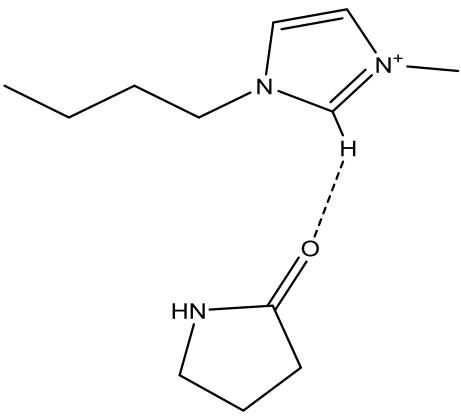

volume of components and has positive or negative sign. The method of calculation of various parameters of the theory based on relevant equations are given elsewhere [45].

The pure components parameters for the PFP theory are included in Table 6. The Flory contact interaction parameter χ_{12}, the only adjustable parameter needed in the PFP theory, was obtained from the experimental V_m^E values in the absence of the experimental excess molar enthalpies $\left(H_m^E\right)$. The Flory contact interaction parameter χ_{12} was found to be negative for all of the investigated temperatures. The values of three contributions: V_{int}^E, V_{fv}^E and V_p^E to V_m^E (PFP), at equimolar compositions are summarized in Table 7. The first term V_{int}^E is negative, which suggests that strong interactions take place in the binary mixtures. The interactional contributions are negative at all temperatures. The second term V_{fv}^E was found to be negative for the system studied (Table 7) as V_{fv}^E is proportional to $-\left(\tilde{V}_1 - \tilde{V}_2\right)^2$ [41]. The magnitude of negative values for V_{fv}^E depends upon difference between Flory's reduced volumes of the components. Negative values of V_{fv}^E increase in magnitude as the temperature increases, which shows that as the temperature increases, more free volume in [Bmim][PF_6] becomes available to accommodate the smaller PY molecules that resulted in the more negative V_m^E values. For the third term, the characteristic pressure effect $V_{p^*}^E$, the P^* effect which depends on the relative cohesive energy of the expanded and less expanded component, is found to be positive at all investigated temperatures. It is proportional to $\left(\tilde{V}_1 - \tilde{V}_2\right)\left(p_1^* - p_2^*\right)$ and can have both the negative and positive sign depending upon the magnitude of p_i^* and $\tilde{V}_i^*$ of the unlike components [45]. For the system [Bmim][PF_6] + PY, V_{p*}^E is positive which is related to the structure-braking effect of PY on the electrostatic interactions between the ions of [Bmim][PF_6], and so the PY molecules can be placed around the $[Bmim]^+$ and $[PF_6]^-$ ions [41, 45]. In the present system, V_{int}^E and V_{fv}^E are found to be negative while $V_{p^*}^E$ is found to be positive which shows that the interaction and free volume contributions are responsible for the overall strong interactions between solute and solvent molecules. We can conclude that it is possible to explain the volumetric behavior of [Bmim][PF_6] + PY binary mixtures quite successfully by application of the PFP theory.

Table 6 Characteristic and reduced parameters for the pure components, used in PFP theory, at various temperatures

T (K)	$\tilde{V}$	V_1^* (10^{-6} $m^3 \cdot mol^{-1}$)	p_1^* (10^{-6} $J \cdot mol^{-1}$)
[Bmim][PF_6]			
303.15	1.1653	178.71	608.45
308.15	1.1676	178.91	609.14
313.15	1.1699	179.11	609.77
318.15	1.1722	179.31	610.35
323.15	1.1745	179.51	610.82
PY			
303.15	1.1949	64.57	761.40
308.15	1.1982	64.63	762.79
313.15	1.2015	64.70	764.08
318.15	1.2048	64.76	765.04
323.15	1.2081	64.83	765.82

Table 7 PFP interaction parameter, χ_{12}, and calculated values of the three contributions from the PFP theory at equimolar composition for the ([Bmim][PF_6] + PY) system at T = (303.15–323.15) K

T (K)	χ_{12} (10^6 J·m^{-3})	V_m^E(int)	$V_m^E(fv)$ (10^{-6} m^3·mol^{-1})	V_m^E(ip)
303.15	− 61.8168	− 0.6938	− 0.0371	0.1754
308.15	− 63.2611	− 0.7233	− 0.0396	0.1820
313.15	− 64.8821	− 0.7556	− 0.0423	0.1888
318.15	− 66.5222	− 0.7890	− 0.0451	0.1954
323.15	− 68.1638	− 0.8233	− 0.0480	0.2021

4 Conclusions

In this study, measured densities, ultrasonic speeds of sound and refractive indices for binary liquids of [Bmim][PF_6] with PY over the entire composition range at temperatures (303.15, 308.15, 313.15, 318.15 and 323.15) K at atmospheric pressure have been used to compute excess/deviation properties. The observed excess values clearly reflect the dominance of strong attractive forces in IL rich region. The attractive forces are further increased with rise in temperature. The IR spectral studies also support inferences drawn from the excess properties. The more acidic C_2–H of the imidazolium cation plays a major role in the formation of hydrogen a bond with the carbonyl oxygen of PY. It was observed that the cyclic dimer in the PY rich region is responsible for the expansion of volume and contraction in the IL rich region because of hydrogen bond formation between the ionic liquid [Bmim][PF_6] and PY. The PFP theory was able to explain the volumetric behavior of the system quite successfully.

References

1. Greaves, T.L., Drummond, C.J.: Proticionic liquids: evolving structure–property relationships and expanding applications. Chem. Rev. **115**, 11379–11448 (2015)
2. Guo, F., Zhang, S., Wang, J., Teng, B., Zhang, T., Fan, M.: Synthesis and applications of ionic liquids in clean energy and environment: a review. Curr. Org. Chem. **19**, 455–468 (2014)
3. Shamsuri, A.A., Daik, R.: Applications of ionic liquids and their mixtures for preparation of advanced polymer blends and composites: a short review. Rev. Adv. Mat. Sci. **40**, 45–59 (2015)
4. Comminges, C., Barhdadi, R., Laurent, M., Troupel, M.: Determination of viscosity, ionic conductivity, and diffusion coefficients in some binary systems: ionic liquids + molecular solvents. J. Chem. Eng. Data **51**, 680–685 (2006)
5. Zhang, P., Peng, L., Li, W.: Application of ionic liquid [bmim]PF_6 as green plasticizer for poly(L-lactide). e-Polymers **172**, 8 (2008)
6. Lin, J., Teng, Y., Lu, Y., Lu, S., Hao, X., Cheng, D.: Usage of hydrophobic ionic liquid [BMIM][PF_6] for recovery of acid dye from wastewater and sequential application in Tussah silk dyeing clean. Soil Air Water **42**, 799–803 (2014)
7. Flieger, J.: Effect of ionic liquids as mobile-phase additives on chromatographic parameters of neuroleptic drugs in reversed-phase high-performance liquid chromatography. Anal. Lett. **42**(11), 1632–1649 (2009)
8. Zhao, H., Sanjay, M.: Applications of ionic liquids in organic synthesis. Aldrichimica Acta **35**(3), 75–83 (2002)
9. Han, D., Ho Row, K.: Recent applications of ionic liquids in separation technology. Molecules **15**, 2405–2426 (2010)

10. Markus, E., Anita, J.M., Alan, J.R.: Enzymatic catalysis of formation of Z-aspartame in ionic liquid—an alternative to enzymatic catalysis in organic solvents. Biotechnol. Prog. **16**, 1129–1131 (2000)
11. Mehta, S.K., Ram, G., Bhasin, K.K.: Effect of placement of hydroxyl groups in isomeric butanediol on the behaviour of thermophysical and spectroscopic properties of pyrrolidin-2-one. J. Chem. Thermodyn. **37**, 791–801 (2005)
12. Garcia, B., Alcalde, R., Leal, J.M., Matos, J.S.: Solute–solvent interactions in amide–water mixed solvents. J. Phys. Chem. **101**, 7991–7997 (1997)
13. Geng, Y., Wang, T., Yu, D., Peng, C., Liu, H., Hu, Y.: Densities and viscosities of the ionic liquid [C4mim][PF6]–*N*, *N*-dimethylformamide binary mixtures at 293.15 to 318.15 K. Chin. J. Chem. Eng. **16**, 256–262 (2008)
14. Fan, W., Zhou, Q., Sun, J., Zhang, S.: Density, excess molar volume, and viscosity for the methyl methacrylate-1-butyl-3methylimidazolium hexafluorophosphate ionic liquid binary system at atmospheric pressure. J. Chem. Eng. Data **54**, 2307–2311 (2009)
15. Zhu, A., Wang, J., Han, L., Fan, M.: Measurements and correlation of viscosities and conductivities for the mixtures of imidazolium ionic liquids with molecular solutes. Chem. Eng. J. **147**, 27–33 (2009)
16. Taghi Zafarani-Moattar, M., Majdan-Cegincara, R.: Viscosity, density, speed of sound, and refractive index of binary mixtures of organic solvent + ionic liquid, 1-butyl-3-methylimidazolium hexafluorophosphate at 298.15 K. J. Chem. Eng. Data **52**, 2359–2364 (2007)
17. Qiao, Y., Fangyou, Y., Xia, S., Shen, Y., Peisheng, M.: Densities and viscosities of [Bmim][PF_6] and binary dystems [Bmim][PF6]–ethanol, [Bmim][PF_6]–benzene at several temperatures and pressures: determined by the falling-ball method. J. Chem. Eng. Data **56**, 2379–2385 (2011)
18. Srinivasa Krishna, K.T., Raju, K.T.S.S., Gowrisankar, M., Anil, K.N., Munibhadrayya, B.: Volumetric, ultrasonic and spectroscopic studies of molecular interactions in binary mixtures of 1-butyl-3-methylimidazolium hexafluorophosphate with 2-propoxyethanol at temperatures from 298.15 to 323.15. J. Mol. Liquids **216**, 484–495 (2016)
19. Armarego, W.L., Chai, C.L.L.: Purification of Laboratory Chemicals. Butterworth-Heinemann publisher, Oxford (2013)
20. Scholz, E.: Karl Fisher Titration. Springer, Berlin (1984)
21. Costa, A.J., Esperanca, I.M., Marrucho, J.M., Rebelo, L.P.N.: Densities and viscosities of 1-ethyl-3-methylimidazolium *n*-alkyl sulfates. J. Chem. Eng. Data **56**, 3433–3441 (2011)
22. Pereiro, A.B., Legido, J.L., Rodriguez, A.: Physical properties of ionic liquids based on 1-alkyl-3-methylimidazolium cation and hexafluorophosphate as anion and temperature dependence. J. Chem. Thermodyn. **39**, 1168–1175 (2007)
23. Troncoso, J., Cerdeiriña, C.A., Sanmamed, Y.A., Romani, L., Lui Rebelo, L.P.N.: Thermodynamic properties of imidazolium-based ionic liquids: densities, heat capacities, and enthalpies of fusion of [bmim][PF_6] and [bmim][NTf_2]. J. Chem. Eng. Data **51**, 1856–1859 (2006)
24. Reid, R.C., Prausnitz, J.M., Poling, B.E.: The Properties of Gases and Liquids, 4th edn, p. 139. McGraw Hill Inc, New York (1987)
25. Srinivasa Krishnaa, T., Anil, K.N., Chentilnathc, S., Punyaseshadud, D., Munibhadrayya, B.: Densities, ultrasounds, refractive indices, excess and partial molar properties of binary mixtures of imidazolium based ionic liquid with pyrrolidin-2-one at temperatures from 298.15 L to 323.15 K. J. Chem. Eng. (2016). https://doi.org/10.1016/j.jct.2016.05.021
26. García, B., Hoyuelos, F.J., Alcalde, R., Leal, J.M.: Molar excess volumes of binary liquid mixtures: 2-pyrrolidinone with C6–C10 *n*-alkanols. Can. J. Chem. **74**, 121–127 (1996)
27. Reddy, M.S., Md Nayeem, S., Soumini, C., Raju, K.T.S.S., Babu, B.H.: Study of molecular interactions in binary liquid mixtures of [Emim][BF_4] with 2-methoxyethanol using thermo acoustic, volumetric and optical properties. Thermochim. Acta **630**, 37–39 (2016)
28. Reddy, M.S., Raju, K.T.S.S., Rao, A.S., Sharmila, N., Babu, B.H.: Study of thermophysical properties of the binary mixtures of ionic liquid 1-ethyl-3-methylimidazolium ethylsulfate and 2-propoxyethanol from T = (298.15 to 328.15) K at atmospheric pressure. J. Chem. Thermodyn. **101**, 139–149 (2016)
29. Reddy, M.S., Md Nayeem, S., Raju, K.T.S.S., Babu, B.H.: The study of solute–solvent interactions in 1-ethyl-3-methylimidazolium tetrafluoroborate + 2-ethoxyethanol from density, speed of sound, and refractive index measurements. J. Therm. Anal. Calorim. **124**, 959–971 (2016)
30. Ali, A., Nabi, F., Tariq, M.: Volumetric, viscometric, ultrasonic, and refractive index properties of liquid mixtures of benzene with industrially important monomers at different temperatures. Int. J. Thermophys. **30**, 464–474 (2009)
31. Reddy, M.S., Raju, K.T.S.S., Md Nayeem, S., Khan, I., Krishna, K.B.M., Babu, B.H.: Excess thermodynamic properties for binary mixtures of ionic liquid 1-ethyl-3-methylimidazolium ethyl sulfate and 2-methoxyethanol from T = (298.15 to 328.15) K at atmospheric pressure. J. Solution Chem. **45**, 675–701 (2016)

32. Roth, C., Appelhagen, A., Jobst, N., Ludwig, R.: Microheterogeneities in ionic-liquid–methanol solutions studied by FTIR spectroscopy, DFT calculations and molecular dynamics simulations. Chem. Phys. Chem. **13**, 1708–1717 (2012)
33. Aggarwal, A., Lancaster, N.L., Sethi, A.R., Welton, T.: The role of hydrogen bonding in controlling the selectivity of Diels–Alder reactions in room-temperature ionic liquids. Green Chem. **4**, 517–520 (2002)
34. Znamenskiy, V., Kobrak, M.N.: Molecular dynamics study of polarity in room-temperature ionic liquids. J. Phys. Chem. B **108**, 1072–1079 (2004)
35. Dhumal, N.R., Kim, H.J., Kiefer, J.:Electronic structure and normal vibrations of the 1-ethyl-3-methylimidazolium ethyl sulfate ion pair. J. Phys. Chem. A **115**, 3551–3558 (2011)
36. Lassegues, J.C., Grondin, J., Cavagnat, D., Johansson, P.: New interpretation of the CH stretching vibrations in imidazolium-based ionic liquids. J. Phys. Chem. A **113**, 6419–6421 (2009)
37. Lassegues, J.C., Grondin, J., Cavagnat, D., Johansson, P.: Reply to the comment on 'New interpretation of the CH stretching vibrations in imidazolium-based ionic liquids'. J. Phys. Chem. A **114**, 687–688 (2009)
38. Grondin, J., Lassegues, J.C., Cavagnat, D., Buffeteau, T., Johansson, P., Holomb, R.: Revisited vibrational assignments of imidazolium-based ionic liquids. J. Raman Spectrosc. **42**, 733–743 (2011)
39. Maria, J.D.V., Rafael, A., Santiago, A.: Pyrrolidone derivatives in water solution: an experimental and theoretical perspective. Ind. Eng. Chem. Res. **48**, 1036–1050 (2009)
40. Vercher, E., Llopis, F.J., Gonzalez-Alfaro, M.V., Andreu, A.M.: Density, speed of sound, and refractive index of 1-ethyl-3-methylimidazolium trifluoromethanesulfonate with acetone, methyl acetate, and ethyl acetate at temperatures from (278.15 to 328.15) K. J. Chem. Eng. Data **55**, 1377–1388 (2010)
41. Patterson, D., Delmas, G.: Corresponding states theories and liquid models. Discuss. Faraday Soc. **49**, 98–105 (1970)
42. Torres, R.B., Ortolan, M.I., Volpe, P.L.O.: Volumetric properties of binary mixtures of ethers and acetonitrile: experimental results and application of the Prigogine–Flory–Patterson theory. J. Chem. Thermodyn. **40**, 442–459 (2008)
43. Flory, P.J.: Statistical thermodynamics of liquid mixtures. J. Am. Chem. Soc. **87**, 1833–1838 (1965)
44. Abe, A., Flory, P.J.: The thermodynamic properties of mixtures of small, nonpolar molecules. J. Am. Chem. Soc. **87**, 1838–1846 (1965)
45. Vaid, Z.S., More, U.U., Oswal, S.B., Malek, N.I.: Experimental and theoretical excess molar properties of imidazolium based ionic liquids with isomers of butanol. Thermochim. Acta **634**, 38–47 (2016)